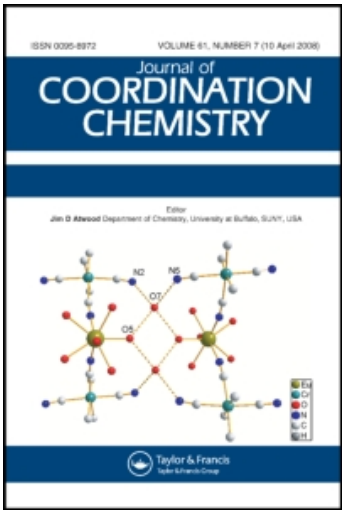

Journal of Coordination Chemistry
Publication details, including instructions for authors and subscription information:
http://www.informaworld.com/smpp/title~content=t713455674

Nickel(II) complexes of tricyclic N_{10}-cage ligands

Ankur Rastogi[a]; Anurag[a]; Ram Nayan[a]
[a] Department of Chemistry, Hindu College, Moradabad 244001, India

First published on: 19 February 2010

To cite this Article Rastogi, Ankur , Anurag and Nayan, Ram(2010) 'Nickel(II) complexes of tricyclic N_{10}-cage ligands', Journal of Coordination Chemistry, 63: 4, 665 — 679, First published on: 19 February 2010 (iFirst)
To link to this Article: DOI: 10.1080/00958971003637059
URL: http://dx.doi.org/10.1080/00958971003637059

Journal of Coordination Chemistry
Vol. 63, No. 4, 20 February 2010, 665–679

Taylor & Francis
Taylor & Francis Group

Nickel(II) complexes of tricyclic N_{10}-cage ligands

ANKUR RASTOGI, ANURAG and RAM NAYAN*

Department of Chemistry, Hindu College, Moradabad 244001, India

(*Received 18 July 2009; in final form 12 October 2009*)

Macrocyclic ligands, 2,5,8,10,13,16,17,20,21,24-decaazatricyclo[7.7.4.4]tetracosane (DATT), 2,5,8,10,13,16,17,20,22,26-decaazatricyclo[7.7.5.5]hexacosane (DTCH), 2,5,8,11,14,17,19,22,23,26-decaazatricyclo[8.8.4.4^{9,18}]hexacosane (DATH), and 2,5,8,11,14,17,19,23,24,28-decaazatricyclo[8.8.5.5^{9,18}]octacosane (DATO), from template condensation of diethylenetriamine with nickel(II) complexes of macrocycles 1,3,6,8-tetraaza-2,2,7,7-tetrachlorocyclodecane (TTCE), 1,3,7,9-tetraaza-2,2,8,8-tetrachlorocyclododecane (TTDE), 1,4,7,10-tetraaza-2,3,8,9-tetrachlorocyclododecane (TTCD), and 1,4,8,11-tetraaza-2,3,9,10-tetrachlorocyclotetradecane (TTTE), respectively, are described. Formulations of the tricyclic cage ligands and their nickel(II) complexes have been confirmed by elemental analyzes, conductivity and potentiometric measurements, and infrared, electronic, ^{1}H-NMR, and mass spectral studies. Highest enhancement of equilibrium constant for nickel(II) complex of DATT (by 10^{10}) over that of the corresponding tetraaza macrocycle of similar planar cavity ([10]-N_4) is observed. The cage effect on equilibrium constant decreases rapidly with increase in planar cavity size ([10]-$N_4 \rightarrow$ [14]-N_4) of the tricyclic ligand; it can be considered negligible in the DATO system where nickel is well fitted in the planar cavity. A small variation in metal-ligand stability constants ($\log K = 21$–23) indicates that a low value due to poor fitting of the nickel in the planar cavity is compensated by its encapsulation in the small spherical cavity. Thus, high and comparable stability constant values are expected for planar tetraaza and spherical polyaza cavity systems in which nickel ion can be nicely fitted.

Keywords: Nickel(II) complexes; Cage ligands; Potentiometric measurements

1. Introduction

Metal complexes of mono-, bi-, and polycyclic macrocycles with tetra [1–7] or poly [8–11] donors have demonstrated quite unusual spectral, thermodynamic, or structural properties. Polydentate cage ligands provide a sterically controlled coordination cavity such that the complexes with unusual properties might result. Considerable efforts have been made to design macrobicyclic cryptands [12–16], which form very stable complexes with various metal cations contained within the central molecular cavity of the cryptand. Graf and Lehn [17] reported a tricyclic cage ligand with molecular formula $C_{24}H_{48}N_4O_6$ [$(18)_4$-O_6N_4] that contains four bridgehead nitrogens and encapsulates NH_4^+ [18]. Polyether cryptands have unique applications in cation recognition, transport, and catalysis. Additional features can arise from other tricyclic cage systems,

*Corresponding author. Email: ramnayan_2003@yahoo.co.in

ISSN 0095-8972 print/ISSN 1029-0389 online
DOI: 10.1080/00958971003637059

particularly consisting of aza groups where donors can effectively encapsulate the guest cation. Many aza-cryptand hosts for transition and main group cations have also been reported [19]. Brooker *et al*. [20] studied complexes of a host derived from "cap unit" tris(2-aminoethyl)amine and "head unit" 3,6-diformylpyridazine which have a variety of exciting properties, including unusual magnetic and redox behavior. This pyridazine spaced Schiff-base ligand also acts as a binucleating host for hexa- or hepta-coordinate cations. A polyaza cage 2,5,8,10,13,16,17,20,23-nonaazabicyclo[7.7.7]tricosane generated in template condensation of diethylenetriamine with trichloromethane coordinates three copper(II) ions in its cavity [21].

Two nitrogens of cryptand participate in the bond formation along with oxygen donors. Since the ligands have 3-D arrangement of binding sites, stability constants are usually higher than those of similar 2-D ligand [22]. The values on average are a factor $\sim 10^3$ larger for the alkali metal [2.2.2] cryptates as compared to alkali metal 18-crown-6 complexes in water. Lehn *et al*. [14] noted a remarkable increase in the stability of the complexes formed by similar planar macrocycle with the cryptate effect on stability more pronounced than that described as the macrocyclic effect. The effect is of enthalpic origin [23, 24]. Aza macrocycles are particularly effective in complexing transition metal ions, but very few log K values are available for nickel binding to macrocycles of this type.

Here, we report the template syntheses and stability of a new category of nickel(II) complexes of four tricyclic N_{10}-cages. The cages 2,5,8,10,13,16,17,20,21,24-decaazatricyclo-[7.7.4.4]tetracosane (DATT), 2,5,8,10,13,16,17,20,22,26-decaazatricyclo[7.7.5.5]-hexacosane (DTCH), 2,5,8,11,14,17,19,22,23,26-decaazatricyclo[8.8.4.$4^{9,18}$]hexacosane (DATH), and 2,5,8,11,14,17,19,23,24,28-decaazatricyclo[8.8.5.$5^{9,18}$]octacosane (DATO) are generated by the condensation of earlier reported [25] nickel(II) complexes of 1,3,6,8-tetraaza-2,2,7,7-tetrachlorocyclodecane (TTCE), 1,3,7,9-tetraaza-2,2,8,8-tetrachlorocyclododecane (TTDE), 1,4,7,10-tetraaza-2,3,8,9-tetrachlorocyclododecane (TTCD), and 1,4,8,11-tetraaza-2,3,9,10-tetrachlorocyclotetradecane (TTTE), respectively, with diethylenetriamine (figure 1). The nickel(II) is octahedrally surrounded in the spherical cavity of the cage by six aza groups. The metal-free cage ligands have been prepared and equilibrium studies involving nickel(II) ions have been made by potentiometric measurement in aqueous solution. Cage effect on equilibrium constant over that of the corresponding tetraaza macrocycle of similar planar cavity size has also been described, and it has been concluded that an increase in the cage effect is associated with decrease in the size of the planar cavity.

2. Experimental

2.1. *Chemicals and reagents*

Solvents and reagents were of reagent grade and used without purification. Solutions of 0.1770N NaOH, 0.02159N HNO_3, and 1.0 M KNO_3 were prepared using G.R. grade chemicals. Nickel(II) nitrate solution prepared in aqueous medium was estimated by EDTA titrations [26]. Aqueous solutions of DATT·10HCl, DTCH·10HCl, DATH·10HCl, and DATO·10HCl were prepared by direct weighing.

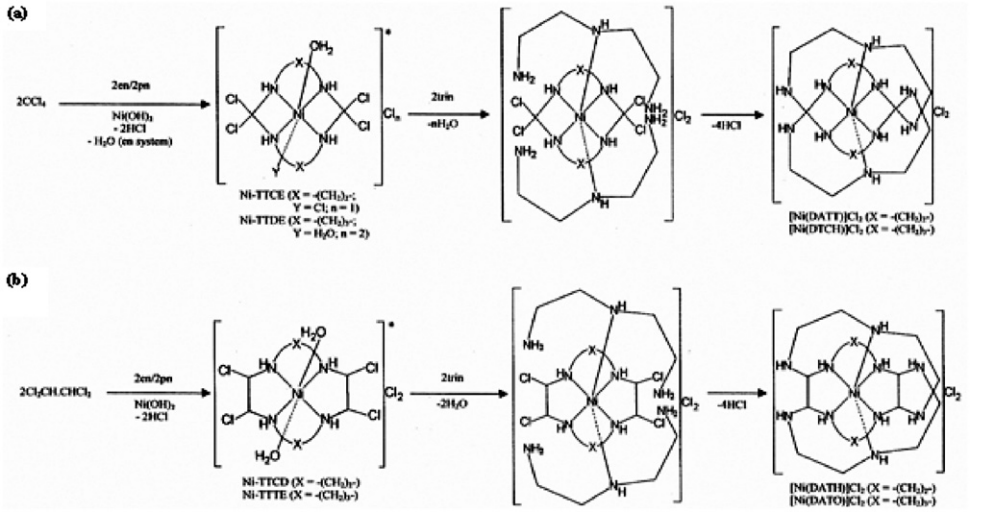

Figure 1. Reaction scheme.
*Reference [25] en=$H_2N{\cdot}CH_2{\cdot}CH_2{\cdot}NH_2$, pn = $H_2N{\cdot}CH_2{\cdot}CH_2{\cdot}CH_2{\cdot}NH_2$, and trin = $H_2N{\cdot}CH_2{\cdot}CH_2{\cdot}NH{\cdot}CH_2{\cdot}CH_2{\cdot}NH_2$.

2.2. *Physical and chemical measurements*

Elemental analyzes were performed by the Central Drug Research Institute, Lucknow. Ionizable chlorides were determined by conductometric titrations [27]. The metal complexes were decomposed and the nickel(II) content was estimated by complexometric titration. A DDR conductivity meter (Type 304) was employed for conductivity measurements. Infrared spectra (FT-IR) from 4000 to 350 cm^{-1} were recorded on a Shimadzu 820 IPC spectrophotometer using KBr disks. Visible electronic spectra of aqueous solutions of the complexes were measured by a Systronic Double Beam Spectrophotometer (2203 Smart). ^{1}H-NMR spectra were run on a Bruker DRX 300 (300 MHz FT) in D_2O solution using DSS as an internal standard. The ESIMS was recorded on a MICROMASS QUATTRO II triple quadrupole mass spectrometer. Sample dissolved in water was introduced into the electrospray ion (ESI) source through a syringe pump at 5 μL per min. The ESI capillary was set at 3.5 KV and the cone voltage was 40 V. The spectrum was collected in 6 s scans and the printouts are average spectra of 6–8 scans.

2.3. *Synthesis of nickel(II) complex of DATT*

A mixture of 1,2-diaminoethane (4.00 g, 66.56 mmol), carbon tetrachloride (10.24 g, 66.57 mmol), and nickel hydroxide (3.08 g, 33.28 mmol) in 200 mL *n*-butanol was refluxed for ~8 h to synthesize [Ni(TTCE)(H_2O)Cl]Cl as reported earlier [25]. Diethylenetriamine (6.86 g, 66.54 mmol) was then added to the condensed mixture with constant stirring and the resulting mixture was further refluxed for 3.7 h during which reddish-brown precipitate changed to light brown, followed by brownish-violet. The whole content was then treated with 100 mL of water. The macrocyclic product was

extracted as red aqueous layer, while negligible amount of brown residue and wine-red non-aqueous layer were rejected. Concentration and refrigeration of the red aqueous solution produced violet crystals with reddish-brown impurity. The impurity was removed by washing the crystals with methanol followed by benzene : ether (1 : 1) and the crystals dried under reduced pressure (yield 6.16 g).

2.4. *Synthesis of nickel(II) complex of DTCH*

Carbon tetrachloride (10.35 g, 67.29 mmol) was added to a stirred mixture of 1,3-diaminopropane (4.99 g, 67.31 mmol) and nickel hydroxide (3.12 g, 33.65 mmol) in 180 mL of *n*-butanol. The mixture was refluxed for ~6 h to yield the product $[Ni(TTDE)(H_2O)_2]Cl_2$, as described earlier [25]. To this cooled mixture, diethylenetriamine (6.94 g, 67.34 mmol) was added with constant stirring. The resulting mixture was refluxed for 1.5 h during which violet precipitate initially formed, changed gradually to bluish-violet. The whole content was then stirred with 100 mL of water and filtered. The wine-red, non-aqueous layer and negligible amount of dark brown residue were rejected and the reddish-violet aqueous layer containing macrocyclic product was concentrated and chilled to crystallize the product. The violet crystals obtained had red sticky impurity. As the impurity was highly soluble in methanol, the crystals were washed with methanol followed by benzene : petroleum ether (1 : 1) and dried (yield 6.69 g).

2.5. *Synthesis of nickel(II) complex of DATH*

In the first step, $[Ni(TTCD)(H_2O)_2]Cl_2$ was synthesized by introducing 3.05 g nickel hydroxide (32.89 mmol) in the reaction mixture of 11.04 g 1,1,2,2-tetrachloroethane (65.77 mmol) and 3.95 g 1,2-diaminoethane (65.72 mmol) in 200 mL *n*-butanol as discussed above. To this cooled mixture, diethylenetriamine (6.78 g, 65.78 mmol) was added slowly with constant stirring giving a violet precipitate and then refluxed for 2.7 h, during which the solution changed to brown (after 15 min), then gradually to dirty brown and finally to red, and the amount of violet precipitate increased. The resulting content was then treated with 100 mL of water and filtered. Bluish-violet aqueous layer was separated from pale-yellow, non-aqueous layer. Concentration and crystallization of the aqueous solution yielded bluish-violet crystals, which were washed with benzene : ether (1 : 1) and dried under reduced pressure (yield 8.21 g).

2.6. *Synthesis of nickel(II) complex of DATO*

A mixture containing 2.50 g nickel hydroxide (26.96 mmol), 4.00 g 1,3-diaminopropane (53.96 mmol), and 2.50 g 1,1,2,2-tetrachloroethane (53.92 mmol) in 200 mL *n*-butanol was refluxed for ~8 h to yield blue nickel-TTTE complex. The mixture was then cooled and 5.56 g of diethylenetriamine (53.94 mmol) was added with constant stirring and further refluxed for ~45 min, during which the color changed from blue to violet. The whole content was then stirred with 100 mL of water and macrocyclic product was separated as violet aqueous layer. The colorless non-aqueous layer was rejected. Concentration and refrigeration of the violet aqueous layer produced violet crystals with pale sticky impurity. This impurity was removed by washing the crystals with benzene : petroleum ether (1 : 1) and the crystals were dried under reduced pressure, yield 7.88 g.

2.7. *Preparation of metal-free macrocycles*

The nickel(II) complexes of DATT (0.88 g, 1.70 mmol), DTCH (0.95 g, 1.66 mmol), DATH (1.17 g, 2.11 mmol), and DATO (1.12 g, 1.89 mmol) were dissolved separately in 50 mL of water and demetallation was achieved by adding concentrated HCl (5 mL, 12N). Concentration and chilling of the resulting solutions yielded crystals of the ligand hydrochlorides DATT·10HCl (white, fine crystals, yield 1.15 g), DTCH·10HCl (white, fine crystals, yield 1.12 g), DATH·10HCl (white, crystalline powder, yield 1.48 g), and DATO·10HCl (white, fine crystals, yield 1.35 g). The crystals were finally washed with ether and dried.

2.8. *Potentiometric titrations*

The mixtures: (i) 0.00126N HNO_3; (ii) 0.001 M DATT·10HCl/DTCH·10HCl/DATH·10HCl/DATO·10HCl + (i); (iii) 0.001 M $Ni(NO_3)_2 \cdot 6H_2O$ + (ii); (iv) 0.001 M Ni-DATO complex + 0.0085 M HCl + (i); (v) 0.001 M Ni-DATT/Ni-DTCH complex + 0.009N HCl + (i); and (vi) 0.001 M Ni-DATH complex + 0.0092N HCl + (i) were titrated pH-metrically at 25°C and at an ionic strength of 0.1 M KNO_3 using a Systronic pH meter (μ pH 362 system) with combined electrode. The initial volume of each mixture was kept at 50 mL. From the experimental data, titration curves (pH *vs.* moles of alkali used per mole of ligand, *a*) were plotted and analyzed [28, 29] to obtain information on metal–ligand equilibria. The titration curve of mixture (iii) coincides with that of mixture (iv), (v), or (vi) of the corresponding ligand system.

3. Results and discussion

3.1. *Synthesis*

Syntheses of mononuclear tetraaza nickel(II) complexes of TTCE, TTDE, TTCD, and TTTE in template condensation between 1,2-diaminoethane and carbon tetrachloride, 1,2-diaminoethane and 1,1,2,2-tetrachloroethane, 1,3-diaminopropane and carbon tetrachloride, and 1,3-diaminopropane and 1,1,2,2-tetrachloroethane, respectively, have been reported [25].

Condensation of two molecules of diethylenetriamine with one molecule of nickel(II) complex of the tetraaza macrocycles TTCE, TTDE, TTCD, or TTTE yields a N_{10}-cage. The two amine molecules coordinate to nickel(II) complex of a tetraaza macrocycle (figure 1) through secondary amine group. Ring closing is then favored involving condensation of the two NH_2 groups of each diethylenetriamine with opposite Cl groups of the nickel coordinated tetraaza macrocycle to generate macrotricyclic N_{10}-cages DATT, DTCH, DATH, and DATO. The nickel(II) is octahedrally coordinated by six aza donors in each macrotricyclic N_{10}-cage cavity. A large increase in the stability constant of nickel complexes of DATT, DTCH, or DATH over that of the similar tetraaza ligand (described under solution stability) supports the cage structure of the macrocycle. The cage effect on stability constant in the DATO system is comparatively low, but since TTCD and TTTE are structurally similar, DATO (derived from TTTE) is also expected to be a tricyclic cage macrocycle like DATH (derived from TTCD).

The structures of the compounds are supported by conductivity measurements, potentiometric studies, elemental analyzes (table 1), IR, ^{1}H-NMR, and mass spectra, etc. Association of HCl with the nickel(II) complexes is confirmed by elemental analyzes, conductivity measurements, IR spectra exhibiting bands due to the protonation of uncoordinated secondary amine group, and by potentiometric studies. These studies show that $[Ni(DATO)]Cl_2{\cdot}1.5HCl{\cdot}0.5H_2O$ is a mixture of diprotonated $[Ni(H_2DATO)]Cl_4$ and monoprotonated $[Ni(HDATO)]Cl_3$ macromolecules, whereas $[Ni(DATH)]Cl_2{\cdot}0.8HCl{\cdot}H_2O$ is a mixture of unprotonated and monoprotonated species. The remaining two complexes are pure monoprotonated macrocyclic compounds. Further, the absence of bands due to free or coordinated primary amine [30–32] in IR spectra of the complexes suggests the formation of condensed macrocyclic ring. The presence of uncoordinated water in the metal complexes was confirmed by heating at 120°C. The loss in weight corresponds to the water in the complex. Metal-free cages and their metal complexes were separately dissolved in water, acidified with HNO_3 and ionizable chlorides were precipitated as AgCl by $AgNO_3$ solution. Precipitate was separated by filtration and rejected, while the filtrate was dried and then fused with sodium to reduce chlorine (if any) bonded covalently to the macrocycle. The resulting sodium extract was found free from chloride.

3.2. *IR spectra*

3.2.1. DATT system. The cyclic nature of $[Ni(DATT)]Cl_2{\cdot}HCl{\cdot}0.5H_2O$ is supported by the presence of bands only due to secondary amine at 3170 (very strong, very sharp), 3266 (very strong and sharp), and 1567 cm^{-1} (medium, very sharp). The first two vibrations are assigned to N–H stretching, while the third is due to bending. Vibrational frequencies at 2919 (strong, sharp), 2874 (strong, very sharp), 1450 (medium, very sharp), and 1090 cm^{-1} (very strong, sharp) are attributed to C–H asymmetric and symmetric stretching, scissoring and ν(C–N) vibrations, respectively. The presence of water is supported by bands at 3439 (strong, sharp), 3322 (shoulder but sharp), and 1624 cm^{-1} (weak), respectively, ascribed to O–H asymmetric and symmetric stretching and bending. Two medium bands at 497 (sharp) and 519 cm^{-1} (very sharp) are assigned to ν(Ni–N).

The IR spectrum of DATT·10HCl shows a very strong but broad band in the region 3100–2800 cm^{-1} assigned to C–H stretching vibrations followed by a series of weak or very weak but generally sharp bands at 2699, 2570, 2438, and 2399 cm^{-1} and a medium, band at 2020 cm^{-1}, due to amine hydrochloride group. The δ(N–H) and δ(C–H) bands appear at 1527 (very strong, very sharp) and 1478 cm^{-1} (strong, sharp), respectively. The N–H stretching vibration is absent, probably coupled with C–H vibrations. The ν(C–N) appears at 1186 cm^{-1}. Other bands in the region 1600–500 cm^{-1} are associated with whole ligand.

3.2.2. DTCH system. The IR spectrum of $[Ni(DTCH)]Cl_2{\cdot}HCl{\cdot}2H_2O$ show vibrations at 3266, 3173, 1568, 2920, 2874, 1449, and 1090 cm^{-1} assigned to ν_1(N–H), ν_2(N–H), δ(N–H), ν_{as}(C–H), ν_s(C–H), δ(C–H), and ν(C–N), respectively. These bands closely resemble bands observed for nickel-DATT complex, due to structural similarity. Two bands at 496 (shoulder but sharp) and 518 cm^{-1} (strong but sharp) are assigned to ν(Ni–N). Bands at 2558 (very weak) and 2106 cm^{-1} (weak) are due to protonated complex. The presence of water is evident by bands at 3442, 3322, and 1624 ascribed to asymmetric, symmetric stretching, and bending modes, respectively.

Table 1. Analytical and physical data for the cage macrocycles.

Compound	Color (color at d.p.)	Yield (%) (m.p. °C)	Λ_M ($Ohm^{-1} cm^2 mol^{-1}$)	% Found (Calcd)					Molecular weight found (Calcd)
				C	H	N	Ni	Cl[b]	
[Ni(DATT)]Cl_2·HCl·0.5H_2O	Violet	39.20	330	32.55	7.00	27.18	11.36	20.49	...
$NiC_{12}H_{36}N_{10}O_{0.5}Cl_3$	(black)	(295)[c]		(32.49)	(7.01)	(27.06)	(11.34)	(20.55)	(517.55)
DATT·10HCl	White	95.04	...	23.85	6.30	19.90	...	50.30	719.00
$C_{14}H_{44}N_{10}Cl_{10}$	(...)	(265)		(23.78)	(6.27)	(19.81)		(50.13)	(707.07)
[Ni(DTCH)]Cl_2·HCl·2H_2O	Violet	39.78	315	33.63	7.59	24.38	10.28	18.64	...
$NiC_{16}H_{43}N_{10}O_2Cl_3$	(gray)	(250)[c]		(33.56)	(7.57)	(24.46)	(10.25)	(18.57)	(572.63)
DTCH·10HCl	White	91.80	...	26.08	6.60	19.12	...	48.38	732.00
$C_{16}H_{48}N_{10}Cl_{10}$	(...)	(200)		(26.14)	(6.58)	(19.05)		(48.22)	(735.12)
[Ni(DATH)]Cl_2·0.8HCl·H_2O	Bluish-violet	50.03	288	35.00	7.50	25.78	10.77	18.06	...
$NiC_{16}H_{40.8}N_{10}OCl_{2.8}$	(black)	(265)[c]		(35.11)	(7.51)	(25.60)	(10.72)	(18.13)	(547.32)
DATH·10HCl	White	95.48	...	26.04	6.60	19.10	...	48.06	732.00
$C_{16}H_{48}N_{10}Cl_{10}$	(...)	(207)		(26.14)	(6.58)	(19.05)		(48.22)	(735.12)
[Ni(DATO)]Cl_2·1.5HCl·0.5H_2O	Violet	55.44	371	36.46	7.55	26.57	9.96	20.88	...
$NiC_{18}H_{44.5}N_{10}O_{0.5}Cl_{3.5}$	(brown)	(290)[c]		(36.52)	(7.58)	(26.66)	(9.92)	(20.96)	(591.89)
DATO·10HCl	White	93.57	...	28.28	6.86	18.39	...	46.31	...
$C_{18}H_{52}N_{10}Cl_{10}$	(brown)[a]	(245)[c]		(28.33)	(6.86)	(18.35)		(46.45)	(763.17)

[a]Melts to brown liquid at 270°C.
[b]Ionizable chloride ions.
[c]Decomposition.

The metal-free ligand hydrochloride spectrum shows a strong and broad band in the region 3100–2800 cm^{-1} ascribed to C–H stretching followed by multiple bands from 2900 to 2200 cm^{-1} with a medium but prominent band at 2023 cm^{-1} assigned to $>NH_2^+$ Cl^- groups, similar to those observed in other amine hydrochloride systems. Bands at 1587 (very strong, sharp), 1485 (strong), and 1172 cm^{-1} (medium, sharp) are attributed to δ(N–H), δ(C–H), and ν(C–N) vibrations, respectively.

3.2.3. DATH system. The bands assigned to stretching and bending modes of water in the nickel complex of DATH are at 3454 (strong and broad) and 1626 cm^{-1} (shoulder), respectively. Strong bands at 2947, 2882, and 1092 and a medium band at 1456 cm^{-1} are attributed to C–H asymmetric, symmetric stretching, ν(C–N) and δ(C–H) modes. The N–H vibrations of secondary amine are at 3171 (strong, very sharp), 3288 (very strong, sharp), and 1591 cm^{-1} (medium) assigned to ν(N–H) and δ(N–H), respectively. The ν(Ni–N) is at 498 (medium but sharp) and 521 cm^{-1} (strong and very sharp). Protonation is evident by weak peaks at 2747, 2363, and 2110 cm^{-1}.

The IR spectrum of metal-free ligand hydrochloride indicates the absence of metal–nitrogen or metal–oxygen bands. In addition, the absence of N–H stretching vibration is due to the coupling with C–H stretching vibrations. The ν(C–H) stretches are very strong but broad in the region 3200–2800 cm^{-1}. The bending N–H and C–H vibrations are strong peaks at 1592 and 1483 cm^{-1}, respectively; ν(C–N) is at 1113 cm^{-1}.

3.2.4. DATO system. The IR spectrum of $[Ni(DATO)]Cl_2{\cdot}1.5HCl{\cdot}0.5H_2O$ shows close correspondence to those of $[Ni(DTCH)]Cl_2{\cdot}HCl{\cdot}2H_2O$, $[Ni(DATH)]Cl_2{\cdot}0.8HCl{\cdot}H_2O$, and $[Ni(DATT)]Cl_2{\cdot}HCl{\cdot}0.5H_2O$, and the spectrum of the metal-free ligand also shows close similarity with other N_{10}-cages.

The O–H stretching and bending modes of vibrations for water in the nickel complex of DATO are at 3444 (strong and sharp) and 1624 cm^{-1} (weak but sharp), respectively. Two bands assigned to ν(N–H) are at 3266 (very strong, sharp) and 3171 (very strong, very sharp), while δ(N–H) is observed at 1566 cm^{-1} (medium but very sharp). Bands at 2918 (strong, very sharp), 2873 (strong, very sharp), and 1449 (medium but very sharp) are ascribed to C–H asymmetric and symmetric stretching and bending vibrations, respectively. The ν(Ni–N) are observed at 519 cm^{-1} (medium but very sharp) and 496 cm^{-1} (weak but sharp). The band at 1090 cm^{-1} (very strong, very sharp) is attributed to ν(C–N).

The metal-free ligand hydrochloride shows a very strong and broad band at 3000–2950 cm^{-1} assigned to C–H stretching followed by a series of weak but generally sharp bands at 2967, 2568, 2436, and 2380 and a medium band at 2018 cm^{-1} due to amine hydrochloride. No band is observed for ν(N–H) while δ(N–H) is at 1528 cm^{-1} (strong, very sharp). The δ(C–H) and ν(C–N) bands are at 1480 (strong, sharp) and 1174 cm^{-1} (weak but sharp), respectively.

3.3. *Comparison of DATO, DATT, DTCH, and DATH cage systems*

Spectra of nickel(II) complex with DATO or DATH are a mixture of two compounds; therefore, the mode of vibrations due to different functional groups recorded for $[Ni(DATO)]Cl_2{\cdot}1.5HCl{\cdot}0.5H_2O$ or $[Ni(DATH)]Cl_2{\cdot}0.8HCl{\cdot}H_2O$ cannot be truly used

for the comparison of bond orders. Hence, only ν(Ni–N) vibration is discussed here to a limited extent.

Hole size calculations based directly on X-ray data, as well as parallel calculations involving molecular mechanics procedures, strongly suggest that 16-membered tetraaza ring provides a cavity, which is near-ideal for nickel [33]. Thus, nickel is not well fitted in the tetraaza planar cavity (*XY*-plane) or it is slightly away from the center of the spherical cavity of 10 aza groups. The nickel may occupy a position in one of the two smaller 3-D cavities of seven aza groups (four in *XY*-plane and three above or below this plane). The ν(Ni–N) vibration energy in nickel complexes with DATT, DTCH, DATH, and DATO follows the order DATH > DATT > DATO > DTCH. The highest frequency for DATH complex is due to its non-protonated species. Further, a higher value for Ni-DATT complex than Ni-DATO or Ni-DTCH complex is probably due to the best fitting of nickel(II) in the smaller 3-D cavity as mentioned above.

3.4. *Electronic spectra*

Electronic spectral measurements have confirmed octahedral geometry of the nickel complexes. The visible electronic spectra of complexes of DATT, DTCH, DATH, and DATO in aqueous solution are virtually identical, indicating that nickel ions are in similar coordination environment. Each spectrum shows three absorption bands at ~12,560, ~18,800, and ~28,820 cm^{-1} ($\epsilon < 3.0$), which are attributed to d–d transition and have been assigned as $^3A_{2g} \rightarrow {}^3T_{2g}$, $^3A_{2g} \rightarrow {}^3T_{1g}$ (F), and $^3A_{2g} \rightarrow {}^3T_{1g}$ (P) of octahedral nickel(II) [34].

3.5. *^{1}H-NMR spectra*

The ^{1}H-NMR spectra of the hydrochloride of each ligand exhibit a singlet at 4.80 ppm, which is expected for ($NH_2^+ + CH$) resonances. Two multiplets in the regions 3.68–3.63 and 3.59–3.54, 3.59–3.55 and 3.50–3.46, 3.60–3.55 and 3.51–3.46, and 3.56–3.54 and 3.49–3.48 ppm in spectra of DATT, DTCH, DATH, and DATO hydrochlorides, respectively, are due to protons of non-equivalent CH_2 groups. The proton resonances shift upfield, due to the successive addition of CH or CH_2 group. Thus, bands (ppm) follow the order: DATT > DTCH ~ DATH > DATO.

3.6. *Mass spectra*

The mass spectra (ESIMS) obtained for DATT·10HCl, DATH·10HCl, and DTCH·10HCl and related molecular fragmentation pattern have been very useful in completing the characterization of the cage macrocycles. A representative mass spectrum of DTCH·10HCl and the corresponding molecular fragmentation are given in 'Supplementary material'. The spectra have been further analyzed on the basis of isotopic abundance of different nuclei, particularly that of chlorine and the most abundant peak has been taken into consideration. The spectra of DTCH·10HCl, DATT·10HCl, and DATH·10HCl exhibit peaks at *m/z* 732, 719, and 738 attributable to the molecular ions $[M-2H]^+$, $[M+13H]^+$, and $[M+4H]^+$, respectively. The isotopic distribution for these molecular ions cannot be analyzed as the intensity of the peaks is very weak [32, 35, 36]. Also, the peaks at *m/z* 698 and 694 for $[M-8H]^+$ and $[M-HCl-4H]^+$ ions in the DATT·10HCl and DATH·10HCl spectra, respectively, do

not show isotopic distribution due to similar reason. The isotopic peaks for most of the other fragments associated with the HCl molecules can be seen in the spectra. In DTCH system, the fragment ion $[M-2HCl+7H]^+$ at *m/z* 669 shows isotopic distribution at *m/z* 665 (35.7%), 667 (90%), 669 (100%), 671 (63%), 673 (24%), and 675 (6%). The intensity of these peaks also corresponds to the intensity as calculated for isotope abundances for a combination of eight chlorine atoms [37]. The isotope peak intensity in other fragments does not correspond to the calculated intensity, probably due to spurious contributions from protonated molecular ions or weak background peaks [37]. But, as the number of chlorine atoms increases in the fragment, the number of peaks increases. Thus, the number of chlorine atoms/HCl molecules can be recognized from the isotopic distribution exhibited by the spectrum. The number of isotopic peaks in fragment ions $[M-3HCl+8H]^+$ and $[M-6HCl-NH-9H]^+$ are six (*m/z* 630–640) and five (*m/z* 490–498), respectively. In fragments $[M-4HCl+H]^+$ and $[M-5HCl-NH-3H]^+$ at *m/z* 589 and 540, respectively, all isotopic peaks are not visible due to their poor intensity.

In the spectrum of DATT·10HCl, peaks that span from *m/z* 665 to 675 (six peaks), from 630 to 640 (six peaks), from 490 to 496 (four peaks), and from 418 to 422 (three peaks) are attributable to $[M-HCl-H]^+$, $[M-2HCl]^+$, $[M-6HCl+5H]^+$ and $[M-8HCl+4H]^+$ ion, respectively. The number of isotope peaks for these fragments corresponds to the peaks as reported for similar number of Cl atoms in literature. Similarly, the DATH·10HCl mass spectrum shows peaks that span from *m/z* 665 to 675 (six peaks), from 490 to 496 (four peaks), from 445 to 447 (two peaks), and 419 and 421 (two peaks) as expected for $[M-2HCl+6H]^+$, $[M-6HCl-NH-9H]^+$, $[M-8HCl+3H]^+$, and $[M-9HCl+13H]^+$ ions, respectively.

All three spectra show peaks corresponding to hydrochloride free ligands at *m/z* 341, 382, and 371 attributable to $[DATT-H]^+$, $[DATH+12H]^+$, and $[DTCH+H]^+$ ions, respectively, further confirming formation of macrocycles. Each spectrum exhibits some common peaks, which are expected for $[C_{10}H_{23}N_7+H]^+$, $[C_{10}H_{21}N_5-4H]^+$, and $[C_4H_{11}N_3+3H]^+$ at *m/z* 243, 207, and 104, respectively. The fragment *m/z* 104 is common in all the systems. The fragments at *m/z* 243 and 207 are common in DATT and DTCH systems due to structural similarity, while the corresponding fragments are different in DATH system. These fragment structures for DATH system are shown below:

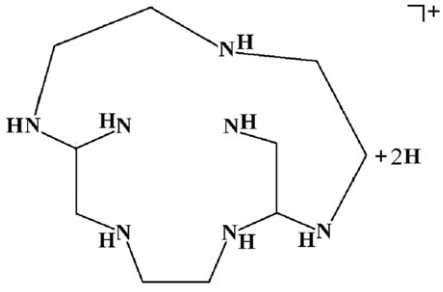

m/z 243

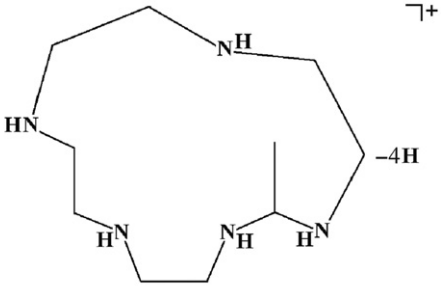

m/z 207

The fragment ions arising from the thermal cleavage of the ligands DATT·10HCl and DATH·10HCl are summarized below:

*DATT·10HCl:*104 $[C_4H_{11}N_3+3H]^+$, 113 $[C_5-H_{11}N_3]^+$, 129 $[C_5H_{12}N_4+H]^+$, 141 $[C_6H_{14}N_4-H]^+$, 158 $[C_7H_{16}N_4+2H]^+$, 181 $[C_8H_{17}N_5-2H]^+$, 207 $[C_{10}H_{21}N_5-4H]^+$,

243 $[C_{10}H_{23}N_7+2H]^+$, 288 $[C_{12}H_{28}N_8+4H]^+$, 303 $[C_{12}H_{29}N_9+4H]^+$, 316 $[C_{13}H_{31}N_9+3H]^+$, 341 $[M-10HCl-H]^+$, 355 $[M-10HCl+13H]^+$, 384 $[M-9HCl+6H]^+$, 418 $[M-8HCl+4H]^+$, 493 $[M-6HCl+5H]^+$, 634 $[M-2HCl]^+$, 669 $[M-HCl-H]^+$.

DATH·10HCl: 104 $[C_4H_{11}N_3+3H]^+$, 181 $[C_8H_{19}N_5-4H]^+$, 207 $[C_{10}H_{21}N_5-4H]^+$, 243 $[C_{10}H_{23}N_7+2H]^+$, 316 $[C_{14}H_{32}–N_8+4H]^+$, 341 $[C_{15}H_{35}N_9]^+$, 355 $[C_{16}H_{37}N_9]^+$, 382 $[M-10HCl+12H]^+$, 419 $[M-9HCl+13H]^+$, 445 $[M-8HCl+3H]^+$, 492 $[M-6HCl-NH-9H]^+$, 668 $[M-2HCl+6H]^+$, 694 $[M-HCl-4H]^+$, 738 $[M+4H]^+$.

3.7. *Solubility, conductivity, and other data*

As ions, the ligand hydrochlorides and their metal complexes are highly soluble in water, but poor in other polar solvents like methanol, ethanol, DMF, and DMSO. The ligands are white and crystalline, but the complexes are violet (crystals) except that of DATH, which is bluish-violet. The molar conductivity values suggest the presence of 0.8 HCl molecules in DATH, 1.0HCl molecules in DATT and DTCH, and 1.5 HCl molecules in DATO complex molecules. The number of ionizable chlorides, recorded in table 1, supports the presence of additional HCl. The $[Ni(DATH)]Cl_2·0.8HCl·H_2O$ and $[Ni(DATO)]Cl_2·1.5HCl·0.5H_2O$ complexes are 2.8 : 1 and 3.5 : 1 electrolytes exhibiting conductance values of 388 and 371 $Ohm^{-1}\,cm^2\,mol^{-1}$, respectively. Conductance values in the range 308–330 $Ohm^{-1}\,cm^2\,mol^{-1}$, determined for $[Ni(DATT)]Cl_2·HCl·0.5H_2O$ and $[Ni(DTCH)]Cl_2·HCl·2H_2O$, are consistent with 3 : 1 electrolytes. All the complexes have decomposition points from 230°C to 295°C. These complexes were heated to 120°C to remove water of crystallization. The metal-free ligand DATO·10HCl decomposes before its melting point at 245°C, whereas remaining ligand hydrochlorides have melting points in the range 190–290°C (table 1).

Table 2. Equilibrium constants for nickel(II) complexes of DATT, DTCH, DATH, and DATO (25°C, $\mu = 0.1$ M KNO_3).

Equilibria number	Reaction[a]	log K			
		DATT system	DTCH system	DATH system	DATO system
(1)	$H_{10}A^{10+} \rightleftharpoons H_9A^{9+} + H^+$	-3.36 ± 0.02	-3.25 ± 0.07	-3.36 ± 0.60	-3.42 ± 0.03
(2)	$H_9A^{9+} \rightleftharpoons H_8A^{8+} + H^+$	-3.68 ± 0.05	-3.67 ± 0.03	-3.59 ± 0.50	-3.96 ± 0.03
(3)	$H_8A^{8+} \rightleftharpoons H_7A^{7+} + H^+$	-3.84 ± 0.03	-3.86 ± 0.06	-3.98 ± 0.80	-5.62 ± 0.02
(4)	$H_7A^{7+} \rightleftharpoons H_6A^{6+} + H^+$	-4.87 ± 0.10	-4.14 ± 0.08	-4.77 ± 0.02	-6.44 ± 0.06
(5)	$H_6A^{6+} \rightleftharpoons H_5A^{5+} + H^+$	-6.87 ± 0.08	-5.97 ± 0.05	-6.64 ± 0.10	-7.02 ± 0.07
(6)	$H_5A^{5+} \rightleftharpoons H_4A^{4+} + H^+$	-7.37 ± 0.06	-7.02 ± 0.10	-7.13 ± 0.09	-7.65 ± 0.05
(7)	$H_4A^{4+} \rightleftharpoons H_3A^{3+} + H^+$	-9.47 ± 0.02	-8.58 ± 0.02	-7.63 ± 0.04	-9.80 ± 0.08
(8)	$H_3A^{3+} \rightleftharpoons H_2A^{2+} + H^+$	-9.93 ± 0.05	-9.75 ± 0.06	-9.67 ± 0.06	-10.10 ± 0.03
(9)	$H_2A^{2+} \rightleftharpoons HA^+ + H^+$	-10.29 ± 0.03	-10.19 ± 0.04	-10.13 ± 0.02	-10.48 ± 0.02
(10)	$HA^+ \rightleftharpoons A + H^+$	-10.55 ± 0.08	-10.36 ± 0.07	-10.56 ± 0.08	-10.86 ± 0.06
(11)	$Ni^{2+} + HA^+ \rightleftharpoons NiHA^{3+}$	19.83 ± 0.12	17.74 ± 0.04	12.46 ± 0.16	22.05 ± 0.18
(12)	$Ni^{2+} + A \rightleftharpoons NiA^{2+}$	21.96 ± 0.17 (11.09)	20.90 ± 0.18 (. . .)	21.20 ± 0.10 (16.40 ± 0.10)	23.11 ± 0.26 (22.20)
(13)	$NiHA^{3+} \rightleftharpoons NiA^{2+} + H^+$	-8.40 ± 0.06	-7.20 ± 0.07	-6.83 ± 0.10	-9.80 ± 0.05

[a]A = DATT/DTCH/DATH/DATO; values in parenthesis represent the values for the corresponding tetraaza macrocycle with similar planar cavity.

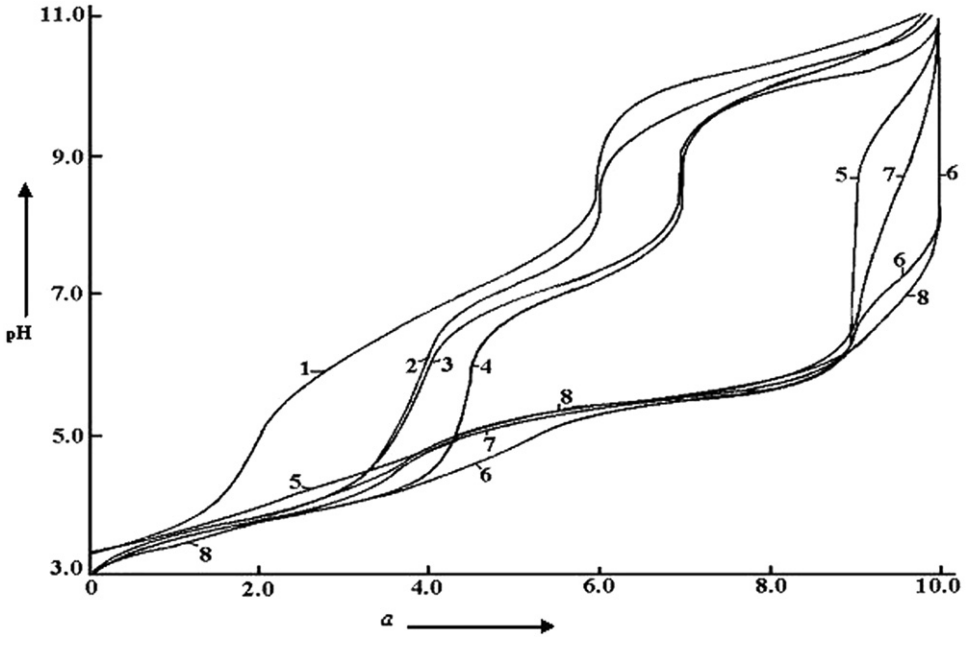

Figure 2. pH *vs.* a curves for N_{10}–cage systems: (1) DATO·10HCl, (2) DATT·10HCl, (3) DATH·10HCl, (4) DTCT·10HCl, (5) Ni^{2+}–DATO·10HCl, (6) Ni^{2+}–DTCH·10HCl, (7) Ni^{2+}–DATT·10HCl and (8) Ni^{2+}–DATH·10HCl (DATO/DATT/DATH/DTCH = 0.001 M).

3.8. *Solution stability*

Proton–ligand equilibria between pH 3.0 and 11.0 (table 2) are shown by titration curves (figure 2) of the hydrochlorides of each N_{10}-cage DTCH, DATT, DATH, or DATO. Four inflections at $a = 3$ (very weak), 4 (steep), 6 (very steep), and 10 (very steep) in the titration curve of DATT hydrochloride indicates that equilibria (1)–(3) below $a = 3$, (5) and (6) between $a = 4$ and 6, and (7)–(10) between $a = 6$ and 10 coexist, whereas the fifth proton independently dissociates from H_6A^{6+} between $a = 4$ and 5. The corresponding curves for DTCH and DATO systems exhibit only two inflections: (DTCH at $a = 4$ (weak) and 7 (steep), and DATO at $a = 2$ (weak) and 6 (very steep)). For DTCH equilibria (1)–(4), below $a = 4$, (5)–(7) between $a = 4$ and 7, and (8)–(10) beyond $a = 7$ also coexist. Similar coexistence of equilibria (1) and (2), (3)–(6), and (7)–(10) is indicated below $a = 2$, between 2 and 6, and 6 and 10, respectively, in the DATO system. A weak inflection at $a = 4$, followed by two-steep inflections at $a = 7$ and 10 is also indicated by titration curves of the DATH system, where equilibria (1)–(4), (5)–(7), and (8)–(10) separately coexist in the different range of a values (figure 2).

Evaluated equilibrium constant values for reactions (1)–(10) are given in table 2. Overall basicity of the N_{10}-cage molecule follows the order: DATO > DATT > DTCH ~ DATH. The highest basicity of DATO is probably due to its flexibility and presence of large number of methylene groups. Flexibility of DATT is reduced compared to that of DTCH, DATH, or DATO. The number of methylene groups in DATT and DATH is small compared to DTCH. Thus, availability of lone pairs is, comparatively, decreased in DATT. However, probably due to its smaller size, solvation is greater making the lone pair available (increased) for protonation.

The formation of $NiHA^{3+}$ in solution is evident from the titration curves of 1 : 1, nickel(II)–ligand systems, which show very weak, steep or very steep inflections at $a \sim 9$ (DATT or DTCH – steep, pH ~ 6.5; DATH – very weak, pH ~ 6 and DATO – very steep, pH ~ 6.4). A gradual color change from green to violet in each titration mixture containing nickel(II) below the pH of inflection also supports their formation. Further increase in a value, up to 10 under the experimental pH condition, shows dissociation of H^+ from the monoprotonated nickel(II) complex $NiHA^{3+}$. The titration curves also exhibit steep or very steep inflections at $a = 10$ at different pH (DATT ~ 10.0, DTCH ~ 7.8, DATH ~ 8.5, and DATO ~ 10.8). No color change beyond $a = 9$ indicates that each non-protonated species is violet. Equilibrium constants for the protonated and non-protonated complexes are reported in table 2. The equilibrium constants for the non-protonated nickel(II) complexes of cages follow the order: DATO > DATT > DATH > DTCH.

Nickel(II) forms mononuclear complex with 1,4,7,11-tetraazacyclotetradecane (cyclam). A high value of equilibrium constant ($\log K = 22.2$ at 25°C, $\mu = 0.1$ M; by spectrophotometric method) for this complex has been reported earlier [38]. The cage DATO, a derivative of cyclam, also forms a nickel(II) complex with enhanced equilibrium constant ($\log K = 23.11$ at 25°C, $\mu = 0.1$ M). Nickel(II) close to the center of the large decaaza spherical cavity is suitably fitted in the planar tetraaza cavity. However, its fitting is poor in the spherical large cavity. About 10 times higher value is attributed to either a poor cage effect or chelate effect due to increase in chelate ring numbers or both. The log K values (~21) for the nickel(II) complexes of DTCH and DATH are comparable because of the similarity in planar cavity ([12]-N_4). A lower value than that for DATO may be because of the reduction in planar cavity size that force the metal to shift from the center of the planar cavity (or center of the large spherical cavity). Thus, metal ion is poorly fitted either in planar or large spherical cavities.

In potentiometric measurement, Thöm and Hancock [39] studied the interaction between nickel(II) cyclen ([12]-N_4 cavity ring) at 25°C and reported the stability constant ($\log K = 16.40 \pm 0.10$) of the complex formed. Here, an increase in the K value for nickel complex of DTCH or DATH over similar tetraaza ligand complex is approximately 10^5; the value is enhanced in DATT in spite of further reduction in the size of planar and spherical cavities as compared to those in DTCH or DATH. The enhancement is probably due to smaller spherical cavity of seven >NH groups (four in XY-plane and three above or below this plane) to a size where the nickel(II) is suitably encapsulated (well fitted) by five >NH groups. The sixth coordination position is occupied by the >NH group of the other cavity and the corresponding metal-nitrogen bond length is slightly larger. The formation constant for nickel(II) complex of 1,3,6,8-tetraazacyclodecane ($\log K = 11.9$) has been recently reported [40]. The cavity size of this [10]-N_4 ligand is equivalent to that of planar cavity of DATT. The enhanced stability of DATT complex over that of this ligand (difference of $\sim 10^{10}$) is due to the cage effect.

In addition to the cavity size effect on stability constant of the nickel complex of the cage macrocycle discussed above, comparatively low solvation of the cage macrocycle can also be responsible for high value of $\log K$ for its metal complex. Similarly, the availability of two additional binding sites in the cage to form an octahedral complex will further increase the stability constant. However, a comparison of increased stability constant value of the nickel complex of the cage macrocycles over that of the

corresponding similar tetraaza planar ligand (cage effect) indicates that major contribution on stability is from the spherical cavity suitable for a nice fit of the cation.

Acknowledgments

We are grateful to UGC, New Delhi, for supporting this work and awarding a fellowship to Ankur Rastogi. The Regional Sophisticated Instrumentation Centre, Punjab University, Chandigarh, and Central Drug Research Institute, Lucknow, are to be thanked for recording the infrared, ^{1}H-NMR, and mass spectra and microanalyzes of the compounds.

References

[1] D.P. Riley, D.H. Busch. *Inorg. Chem.*, **22**, 4141 (1983).
[2] T.N. Mali, P.W. Wade, R.D. Hancock. *J. Chem. Soc., Dalton Trans.*, 67 (1992).
[3] R.D. Hancock, H. Maumela, A.S. de Sousa. *Coord. Chem. Rev.*, **148**, 315 (1996).
[4] S. Sujatha, S. Balasubramanian, H.-K. Fun, K. Chinnakali. *Polyhedron*, **27**, 1925 (2008).
[5] K.P. Guerra, R. Delgado. *Polyhedron*, **27**, 2265 (2008).
[6] S. Chandra, S. Verma, U. Dev, N. Joshi. *J. Coord. Chem.*, **62**, 1327 (2009).
[7] D.L. Maples, R.D. Maples, W.A. Hoffert, T.H. Parsell, A . van Asselt, J.D. Silversides, S.J. Archibald, T.J. Hubin. *Inorg. Chim. Acta*, **362**, 2084 (2009).
[8] P.K. Coughlin, S.J. Lippard. *Inorg. Chem.*, **23**, 1446 (1984).
[9] S. Brooker, T.C. Davidson, S.J. Hay, R.J. Kelly, D.K. Kennepohl, P.G. Plieger, B. Moubarake, K.S. Murray, E. Bill, E. Bothe. *Coord. Chem. Rev.*, **222**, 33 (2001).
[10] S. Sreedaran, K.S. Bharathi, A.K. Rahiman, K. Rajesh, G. Nirmala, L. Jagadish, V. Kaviyarasan, V. Narayana. *Polyhedron*, **27**, 1867 (2008).
[11] A. Bencini, A. Bianchi, A. Danesi, C. Giorgi, P. Mariani, B. Valtancoli. *J. Coord. Chem.*, **62**, 82 (2009).
[12] B. Dietrich, J.M. Lehn, J.P. Sauvage. *Tetrahedron Lett.*, **34**, 2885 (1969).
[13] B. Dietrich, J.M. Lehn, J.P. Sauvage. *J. Chem. Soc., Chem. Commun.*, 15 (1973).
[14] J.M. Lehn, J.P. Sauvage. *J. Am. Chem. Soc.*, **97**, 6700 (1975).
[15] J.M. Lehn, J.P. Simon. *Helv. Chim. Acta*, **60**, 141 (1977).
[16] R.M. Izatt, J.J. Christensen (Eds). *Synthetic Multidentate Macrocyclic Compounds*, Academic Press, New York (1978).
[17] E. Graf, J.M. Lehn. *J. Am. Chem. Soc.*, **97**, 5022 (1975).
[18] B. Metz, J. Rosalky, R. Weiss. *J. Chem. Soc., Chem. Commun.*, 533 (1976).
[19] J. Nelson, V. Mckee, G.G. Morgan. *Prog. Inorg. Chem.*, **47**, 167 (1998).
[20] S. Brooker, J.D. Ewing, J. Nelson. *Inorg. Chim. Acta*, **317**, 53 (2001).
[21] Anurag, A.K. Pandey, R. Nayan. *J. Ind. Chem. Soc.*, **82**, 732 (2005).
[22] J.M. Lehn, J.P. Sauvage, B. Dietrich. *J. Am. Chem. Soc.*, **92**, 2916 (1970).
[23] G. Anderegg. *Helv. Chim. Acta*, **58**, 1218 (1975).
[24] E. Kauffmann, J.M. Lehn, J.P. Sauvage. *Helv. Chim. Acta*, **59**, 1099 (1976).
[25] M. Singh, Anurag, R. Nayan. *Synth. React. Inorg. Met.-Org. Chem.*, **30**, 1703 (2000).
[26] J. Bassett, R.C. Denny, G.H. Jeffery, J. Mendham. *Vogel's Text Book of Quantitative Inorganic Analysis*, 4th Edn, Longman Group Ltd, London (1978).
[27] M. Singh, R. Nayan. *Synth. React. Inorg. Met.-Org. Chem.*, **27**, 619 (1997).
[28] R. Nayan, A.K. Dey. *Indian J. Chem.*, **14A**, 892 (1976).
[29] R. Nayan. *J. Inorg. Nucl. Chem.*, **43**, 3283 (1981).
[30] M.S. Holtman, S.C. Cummings. *Inorg. Chem.*, **15**, 660 (1976).
[31] S.C. Jackels, K. Farmery, E.K. Barefield, N.J. Rose, D.H. Busch. *Inorg. Chem.*, **11**, 2893 (1972).
[32] M. Singh, R. Nayan. *Synth. React. Inorg. Met.-Org. Chem.*, **28**, 87 (1998).
[33] L.F. Lindoy. *The Chemistry of Macrocyclic Ligand Complexes*, Cambridge University Press, Cambridge (1990).
[34] A.B.P. Lever. *Inorganic Electronic Spectroscopy*, 1st Edn, Elsevier, Amsterdam (1968).
[35] Anurag, A.K. Pandey, R. Nayan. *J. Coord. Chem.*, **59**, 1963 (2006).

[36] A. Rastogi, R. Nayan. *J. Coord. Chem*., **62**, 3366 (2009).
[37] B.S. Furniss, A.J. Hannaford, V. Rogers, P.W.G. Smith, A.R. Tatchell. *Vogel's Text Book of Practical Organic Chemistry Including Qualitative Organic Analysis*, 4th Edn, ELBS and Longman Group Ltd, London (1978).
[38] F.P. Hinz, D.W. Margerum. *Inorg. Chem*., **13**, 2941 (1974).
[39] V.J. Thöm, R.D. Hancock. *J. Chem. Soc., Dalton Trans*., 1877 (1985).
[40] A. Rastogi, Anurag, R. Nayan. *J. Indian Chem. Soc*., **86**, 783 (2009).